Effects of Ni substitution for Fe/Co on mechanical and magnetic properties of Co-based bulk metallic glasses

Qianqian Wang [a], Genlei Zhang [a], Jing Zhou [a], Chenchen Yuan [a], Baolong Shen [a, b, *]

[a] School of Materials Science and Engineering, Jiangsu Key Laboratory for Advanced Metallic Materials, Southeast University, Nanjing, 211189, China
[b] Institute of Massive Amorphous Metal Science, China University of Mining and Technology, Xuzhou, 221116, China

ABSTRACT

The influences of Ni substitution for Fe/Co on the thermal, mechanical and magnetic properties of $(Co_{1-x-y}Ni_xFe_y)_{68}B_{21.9}Si_{5.1}Nb_5$ ($x = 0$, $y = 0.3$; $x = 0.1$, $y = 0.2$; $x = 0.2$, $y = 0.1$; $x = 0.3$, $y = 0$; $x = 0.4$, $y = 0$; $x = 0.5$, $y = 0$) metallic glasses are investigated. A new $(Co_{0.5}Ni_{0.5})_{68}B_{21.9}Si_{5.1}Nb_5$ bulk metallic glass (BMG) with a high strength of 4070 MPa and a large plasticity of 3.8% is successfully prepared. The higher Poisson's ratio (ν) increases the effective free volume in the alloy, which promotes plastic flow before fracture. Besides, the lower glass transition temperature indicates lower shear flow barrier, and the narrower supercooled liquid region can easily improve the structural heterogeneity, both of which enhance the plastic strain of the BMG. Furthermore, the effects of the addition of elements that have large ν (Ni) or positive mixing enthalpy with major elements (Cu), as well as their co-addition, on the mechanical properties of CoFeBSiNb BMG system are compared. The substitution of Fe/Co with Ni leads to the decrease of both saturation magnetization and coercivity of the metallic glasses, and the material even changes from ferromagnetic to paramagnetic after Fe is completely replaced by Ni because of the low atomic magnetic moment of Ni. This work not only confirms the universal critical Poisson's ratio for plasticity in Co-based BMGs, but also provides design guidelines for Co-based BMGs with large plasticity.

© 2019 Elsevier B.V. All rights reserved.

1. Introduction

Co-based metallic glasses have excellent magnetic properties, i.e., high saturation magnetization (B_s), high effective permeability (μ_e), low coercivity (H_c), and excellent giant magnetic inductance (GMI) effect, which make them promising functional materials [1,2]. In 2001, a $Co_{43}Fe_{20}Ta_{5.5}B_{31.5}$ bulk metallic glass (BMG) with a critical diameter (D_c) of 2 mm was prepared by copper mold casting, and showed an extremely high strength up to 5190 MPa, which made it possible for the Co-based BMGs to be applied as structural materials [3–5]. Until now, Co-based BMGs with a large glass-forming ability (GFA), e.g. $Co_{42}Cu_1Fe_{20}Ta_{5.5}B_{26.5}Si_5$ BMG having a critical diameter of 6 mm [6], or a super-high fracture strength, e.g. $Co_{55}Ta_{10}B_{35}$ BMG exhibiting a fracture strength of 6020 MPa [7], have been successfully prepared. However, Co-based BMGs may fail catastrophically under loading due to their small room-

temperature plastic strain, which is usually below 2%. The limited room-temperature plasticity not only decreases the reliability of Co-based BMGs, but also makes it difficult to manufacture the ribbons for applications as magnetic materials, such as folding. Thus, it is required to improve the room-temperature plasticity of Co-based BMGs.

It was found that increasing the Poisson's ratio (ν) or decreasing the value of G/B (G and B are shear modulus and bulk modulus, respectively) by tuning the compositions of BMGs is an effective method to improve the plasticity [8–12]. The large global plasticity of $Pt_{57.5}Cu_{14.7}Ni_{5.3}P_{22.5}$ BMG, which is the first monolithic BMG that shows a plastic strain up to 20%, was proposed to be related to its high ν (0.42) and low G/B (0.165) [13]. The high ν and low G/B makes the shear bands to collapse instead of developing into cracks, and thus results in the large plasticity. By comparing the physical and mechanical properties of typical BMGs, Lewandowski et al. revealed a correlation between the fracture energy and the Poisson's ratio, and proposed a critical ν value of 0.31–0.32 for brittle-to-tough transition. Based on this criteria, modulation of the plasticity in several BMG systems has been achieved by changing the Poisson's ratio through composition modification or optimization

---

of processing techniques. The addition of Er or Dy in $Fe_{65}Mo_{14}C_{15}B_6$ BMG sees the onset of plasticity for ν near 0.32 [14]. An increase of ν in $Zr_{56}Co_{28}Al_{16}$ BMG is observed by decreasing the electrical power of the arc during casting, resulting the increase of free volume, and thus the global plasticity is improved [15]. Through molecular dynamics simulation of $Cu_{64}Zr_{36}$ metallic glass, Cheng et al. suggested that the full icosahedral ordering is the key structural feature that controls both the elastic properties including ν and G/B, and the energy barrier and propensity for shear transformations that naturally determines the plastic behavior [16]. Analyses using finite element simulations showed that the higher ν of BMGs can promote the inhomogeneous stress distribution, leading to earlier nucleation and easier arrest of shear bands, and result in larger plastic strain [17]. In a word, obtaining higher ν or lower value of G/B is a promising way to enhance the plasticity of BMGs. However, rare report has been made about the improvement of the plasticity for the Co-based BMGs by modulating their ν or G/B. Therefore, it is of great significance to explore Co-based BMGs with high strength and large ductility by increasing ν or reducing G/B value.

In this work, The $(Co_{0.7}Fe_{0.3})_{68}B_{21.9}Si_{5.1}Nb_5$ BMG with large GFA and high strength but poor plasticity was selected as the base alloy [18]. By substituting Fe/Co with Ni, which has a higher ν (0.31) and lower value of G/B (0.42) than Fe ($\nu = 0.29$ and $G/B = 0.48$) [16], $(Co_{1-x-y}Ni_xFe_y)_{68}B_{21.9}Si_{5.1}Nb_5$ (x = 0, y = 0.3; x = 0.1, y = 0.2; x = 0.2, y = 0.1; x = 0.3, y = 0; x = 0.4, y = 0; x = 0.5, y = 0) BMGs were produced. Besides, the influences of Ni substitution for Fe/Co on the thermal, mechanical and magnetic properties of CoFeBSiNb BMGs were systematically investigated. This study provides useful guidelines to obtain Co-based BMGs with large plasticity.

2. Experimental

Multi-component alloy ingots with nominal atomic compositions $(Co_{1-x-y}Ni_xFe_y)_{68}B_{21.9}Si_{5.1}Nb_5$ (x = 0, y = 0.3; x = 0.1, y = 0.2; x = 0.2, y = 0.1; x = 0.3, y = 0; x = 0.4, y = 0; x = 0.5, y = 0) were prepared by arc melting mixtures of pure Co (99.99 wt%), Fe (99.99 wt%), Ni (99.99 wt%), B (99.999 wt%), Si (99.99 wt%) and Nb (99.95 wt%) in a high purity argon atmosphere. Ribbons with a thickness of 30 μm and a width of 1.2 mm were produced by single roller melt-spinning method. The cylindrical rods with diameters from 1 to 5.5 mm were fabricated by a copper mold casting method. The structure of as-cast alloys was identified by X-ray diffraction (XRD, Bruker D8 Discover) with Cu-$K\alpha$ radiation. The thermal parameters, including glass transition temperature (T_g), crystallization temperature (T_x) and melting temperature (T_m) of the amorphous samples were measured by differential scanning calorimeter (DSC, NETZSCH 404F3) at a heating rate of 0.67 K/s, while liquidus temperature (T_l) was tested by DSC at a cooling rate of 0.067 K/s. The fracture strength (σ_f) and plastic strain (ε_p) were measured by compressive tests at room temperature with a strain rate of 5×10^{-4} s^{-1} using an electromechanical testing machine (Sans 5305). The gauge size of bulk glassy rods for compressive tests was 1 mm in diameter and 2 mm in length. The morphologies of deformed and fractured surfaces were analyzed by scanning electron microscope (SEM, FEI Sirion 200). The B_s was measured using a vibrating sample magnetometer (VSM, Lake Shore 7410) under the maximum applied field of 800 kA/m. The H_c of amorphous ribbons with a length of 70 mm was measured using a DC B-H loop tracer (RIKEN BHS-40) under a maximum field of 800 A/m. The ribbons for magnetic property measurements were annealed for 300 s at specific temperatures (T_g −50 K) for structural relaxation. Nanostructures of the bulk glassy rods were carried out on an transmission electronic microscope (TEM, FEI Tecnai G2 20). The samples for TEM analyses were prepared by ion milling method (Gatan Inc., PIPS-M691) under liquid nitrogen cooling condition.

3. Results and discussion

The D_c of $(Co_{1-x-y}Ni_xFe_y)_{68}B_{21.9}Si_{5.1}Nb_5$ (x = 0, y = 0.3; x = 0.1, y = 0.2; x = 0.2, y = 0.1; x = 0.3, y = 0; x = 0.4, y = 0; x = 0.5, y = 0) BMGs were determined using XRD. Cylindrical rods of each composition were produced in different diameters and analyzed by XRD. The largest diameter of the BMG that has no sharp diffraction peak on the XRD curve is defined as D_c, which is usually taken as the indicator for the GFA of BMGs. As shown in Fig. 1, only broad diffusive peaks can be seen on the XRD curves of the Co-based BMGs with different diameters. Thus, the D_c values of $(Co_{1-x-y}Ni_xFe_y)_{68}B_{21.9}Si_{5.1}Nb_5$ BMGs are 5.5, 5, 4, 2.5, 1.5 and 1.5 mm, respectively. The GFA of this alloy system decreases continuously with increasing Ni content. The reason for the negative influence of Ni on the GFA is uncovered by the analyses from DSC.

The heating DSC traces of the as-cast $(Co_{1-x-y}Ni_xFe_y)_{68}B_{21.9}Si_{5.1}Nb_5$ BMGs are shown in Fig. 2, and the thermal parameters of the BMGs, including T_g, T_x, ΔT ($\Delta T = T_x - T_g$), T_m, T_l and the reduced glass transition temperature T_{rg} ($T_{rg} = T_g/T_l$), are summarized in Table 1. During heating process, all the alloys exhibit one endothermic event, which is the characteristic of the glass transition from the amorphous solid to the supercooled liquid and further confirms the glassy nature of the as-cast rods, followed by exothermic crystallization processes. With increasing Ni content, the T_g and T_x decrease from 854 to 806 K and 896 to 842 K,
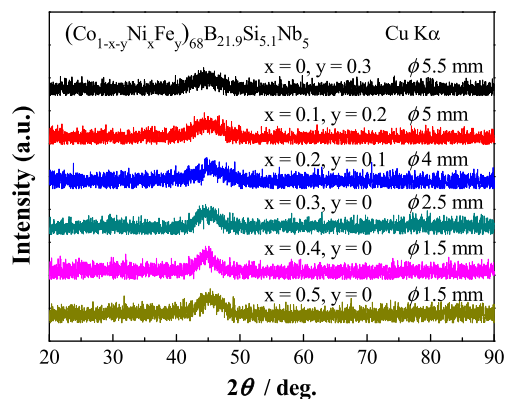

Fig. 1. XRD curves of the as-cast $(Co_{1-x-y}Ni_xFe_y)_{68}B_{21.9}Si_{5.1}Nb_5$ (x = 0, y = 0.3; x = 0.1, y = 0.2; x = 0.2, y = 0.1; x = 0.3, y = 0; x = 0.4, y = 0; x = 0.5, y = 0) rods with critical diameters.

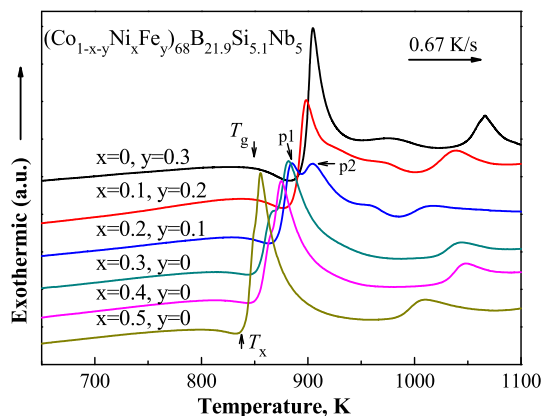**Fig. 2.** DSC traces for the as-cast $(Co_{1-x-y}Ni_xFe_y)_{68}B_{21.9}Si_{5.1}Nb_5$ (x = 0, y = 0.3; x = 0.1, y = 0.2; x = 0.2, y = 0.1; x = 0.3, y = 0; x = 0.4, y = 0; x = 0.5, y = 0) metallic glasses at a heating rate of 0.67 K/s.
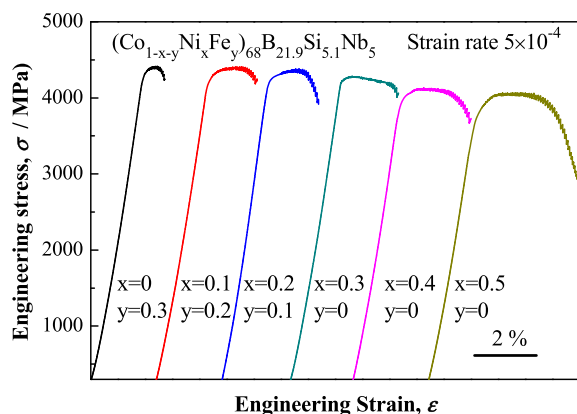
Table 1
Critical diameters, thermal stability, mechanical properties, and magnetic properties of the as-cast $(Co_{1-x-y}Ni_xFe_y)_{68}B_{21.9}Si_{5.1}Nb_5$ (x = 0, y = 0.3; x = 0.1, y = 0.2; x = 0.2, y = 0.1; x = 0.3, y = 0; x = 0.4, y = 0; x = 0.5, y = 0) metallic glasses.

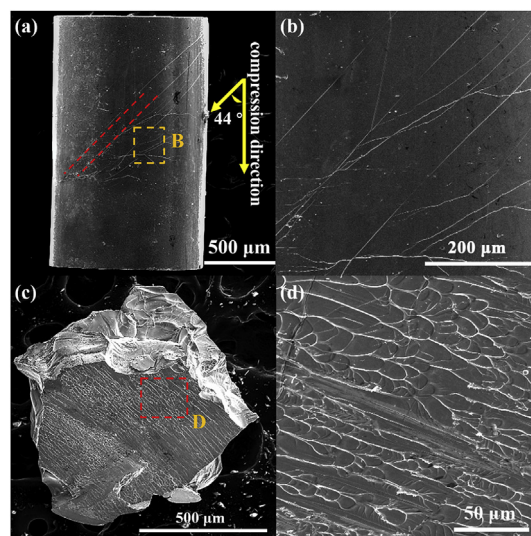| Ni content	T_g (K)	T_x (K)	ΔT (K)	T_m (K)	T_l (K)	T_g/T_l	σ_f (MPa)	ε_p (%)	H_c (A/m)	B_s (T)	D_c (mm)
0	854	896	42	1294	1320	0.65	4415	0.8	0.78	0.70	5.5
0.1	843	885	42	1254	1348	0.63	4410	1.8	0.40	0.51	5.0
0.2	832	873	41	1280	1375	0.61	4385	2.1	0.27	0.20	4.0
0.3	810	851	41	1311	1297	0.62	4280	2.3	–	–	2.5
0.4	809	848	39	1314	1295	0.62	4130	2.7	–	–	1.5
0.5	806	842	36	1314	1283	0.63	4070	3.8	–	–	1.5

respectively. Moreover, the ΔT and T_{rg} of these BMGs decrease gradually from 42 to 36 K and 0.65 to 0.63, respectively, indicating the reduced GFA of the BMG and the decreased thermal stability of the supercooled liquid. Besides, it is noteworthy that when x increases to 0.2, the first two exothermic peaks (indicated by p1 and p2 in Fig. 2) overlap with each other, revealing a competing crystallization process [19]. By further increasing Ni content, p1 disappears gradually. When x = 0.5, p1 is not observed on the DSC anymore, and only p2 exists. These crystallization behaviors suggest that the addition of Ni may induce the formation of some new crystalline phases that are different from the primary crystalline phase in the alloy with x = 0 during heating. This speculation will be confirmed by the results obtained from Fig. 5 in the following section.

The mechanical performance of the $(Co_{1-x-y}Ni_xFe_y)_{68}B_{21.9}Si_{5.1}Nb_5$ BMGs prepared in this work were investigated via compressive tests at room temperature, with the engineering stress-strain curves of the samples shown in Fig. 3. All the samples exhibit super-high strength above 4000 MPa, although a slight decreasing trend is observed with increasing Ni content. In contrast, the plastic strain of these samples increases continuously from 0.8% (x = 0, y = 0.3) to 3.8% (x = 0.5, y = 0). The fracture strength and the plastic strain of the BMGs are also listed in Table 1. The plastic strain of $(Co_{0.5}Ni_{0.5})_{68}B_{21.9}Si_{5.1}Nb_5$ is much larger than that of most Co-based reported BMGs, and it also shows relatively high strength.

The morphologies of deformed and fracture surfaces of the $(Co_{0.5}Ni_{0.5})_{68}B_{21.9}Si_{5.1}Nb_5$ BMG after compressive tests were examined by SEM and shown in Fig. 4, which reveal characteristics of the deformation process of this sample. As shown by the lateral surface of the BMG after deformation (Fig. 4a), the angle between the major fracture surface and loading direction is about 44°. The region B, as indicated by the dashed square in Fig. 4a and enlarged
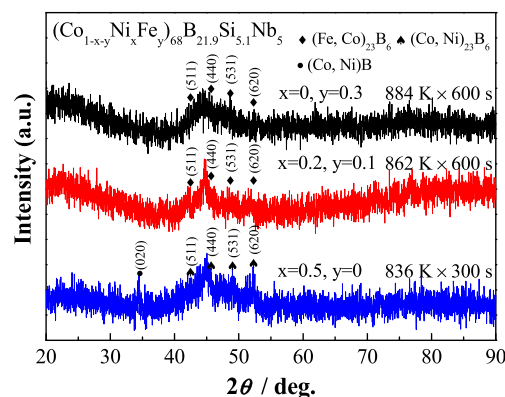

Fig. 4. SEM images of (a) multiple shear bands on the deformed lateral surface and (c) vein pattern on the fracture surface of the $(Co_{0.5}Ni_{0.5})_{68}B_{21.9}Si_{5.1}Nb_5$ BMG; (b) and (d) are the enlarged areas B and D in the (a) and (c), respectively.

in Fig. 4b, shows parallel main shear bands and visible intersecting, branching and arresting of shear bands on the sample surface, indicating the high resistant ability to the propagation of shear bands. The fracture surface of this BMG, as shown in Fig. 4c, together with their partially enlarged details (Fig. 4d), exhibits well-developed vein patterns. Furthermore, vein patterns cross and propagate on cracks, and thus hinder the occurrence of sudden fracture. This phenomenon often reflects the local viscous flow of amorphous alloys and only occurs in the BMGs with good plasticity. The appearance of the vein patterns in the $(Co_{0.5}Ni_{0.5})_{68}B_{21.9}Si_{5.1}Nb_5$

Fig. 3. Compressive stress-strain curves of $(Co_{1-x-y}Ni_xFe_y)_{68}B_{21.9}Si_{5.1}Nb_5$ (x = 0, y = 0.3; x = 0.1, y = 0.2; x = 0.2, y = 0.1; x = 0.3, y = 0; x = 0.4, y = 0; x = 0.5, y = 0) BMGs with diameters of 1 mm.

Fig. 5. XRD patterns of $(Co_{1-x-y}Ni_xFe_y)_{68}B_{21.9}Si_{5.1}Nb_5$ (x = 0, y = 0.3; x = 0.2, y = 0.1; x = 0.5, y = 0) metallic glasses subjected to annealing at 30 K above T_g to determine their primary crystalline phase.
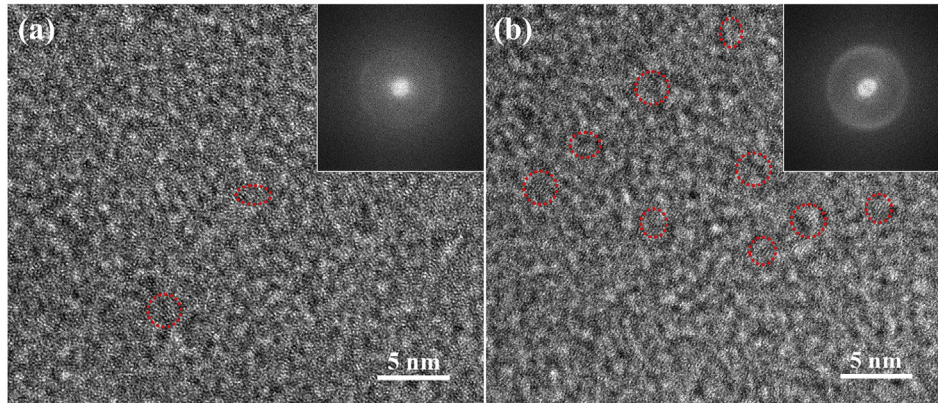
Fig. 6. TEM images of (a) $(Co_{0.7}Fe_{0.3})_{68}B_{21.9}Si_{5.1}Nb_5$ and (b) $(Co_{0.5}Ni_{0.5})_{68}B_{21.9}Si_{5.1}Nb_5$ BMGs. The corresponding SAED patterns are shown in the insets.

evidently verifies its enhanced plasticity. In general, the plastic deformation of BMGs is highly localized into shear bands, followed by the rapid propagation of these shear bands, then the vein patterns are formed during fracture. Consequently, the generation and propagation of high-density multiple shear bands and abundant vein patterns in this Co-based BMG lead to the large plastic deformation.

The origin of the improved plasticity can be explained from the change of ν and G/B value of the BMGs. As Ni and Co have similarly higher ν and lower value of G/B compared with Fe [16], the substitution of Fe/Co with Ni improves the ν and decreases the G/B value of the Co-based BMGs prepared in this work. On the one hand, the increase of the ν value is accompanied by the increase of the effective volume of shear transformation zones (STZs) and the collective motion of STZs leads to the nucleation of shear bands [16,20]. Therefore, BMGs with higher ν value, which means larger STZ volume, can effectively improve the shear deformation ability by generating a larger number of shear bands during deformation. And the high-density multiple shear bands result in large plastic deformation. On the other hand, a small G can promote the propagation of shear bands, while the high B makes the transition from shear bands to cracks more difficult [13,21], indicating better resistance to fracture and easier plastic deformation of the alloy. Consequently, the higher ν and lower value of G/B of the $(Co_{0.5}Ni_{0.5})_{68}B_{21.9}Si_{5.1}Nb_5$ BMG results in its large plasticity.

In addition, the lower T_g and smaller ΔT also plays an important role in improving the plasticity of $(Co_{0.5}Ni_{0.5})_{68}B_{21.9}Si_{5.1}Nb_5$ BMG [22]. As the lower T_g indicates the decrease in shear modulus and lower shear activation energy, the alloys with reduced T_g are more prone to shear deformation [23]. Besides, BMGs with a narrow ΔT are more susceptible to microstructural changes, and easier to induce nanocrystals or nanoclusters on amorphous matrix, in another word, easier to improve the structural heterogeneity [24]. It is well accepted that the structural heterogeneity can modulate the plastic strain of BMGs effectively [25−28]. In order to verify this theory, we carried out isothermal annealing experiments in the supercooled liquid region of the metallic glasses. Fig. 5 shows the XRD curves of $(Co_{1-x}Ni_xFe_y)_{68}B_{21.9}Si_{5.1}Nb_5$ ($x = 0$, $y = 0.3$; $x = 0.2$, $y = 0.1$; $x = 0.5$, $y = 0$) metallic glasses annealed at 30 K above T_g to determine their primary crystalline phases. The primary crystalline phase of the $(Co_{0.7}Fe_{0.3})_{68}B_{21.9}Si_{5.1}Nb_5$ and $(Co_{0.7}Ni_{0.2}Fe_{0.1})_{68}B_{21.9}Si_{5.1}Nb_5$ metallic glasses is $(Co, Fe)_{23}B_6$ resulting from the construction of a network-like structure, which leads to high stability of supercooled liquid against crystallization [29,30]. However, in the $(Co_{0.5}Ni_{0.5})_{68}B_{21.9}Si_{5.1}Nb_5$ metallic glass, not only $(Co, Ni)_{23}B_6$ but also $(Co, Ni)B$ phases are observed, indicating a

competitive crystallization process. Furthermore, it only takes 300 s for the initiation of crystallization in $(Co_{0.5}Ni_{0.5})_{68}B_{21.9}Si_{5.1}Nb_5$ metallic glass, compared with the 600 s for the $(Co_{0.7}Fe_{0.3})_{68}B_{21.9}Si_{5.1}Nb_5$ and $(Co_{0.7}Ni_{0.2}Fe_{0.1})_{68}B_{21.9}Si_{5.1}Nb_5$ metallic glasses. In a word, the lower T_g and the smaller ΔT in $(Co_{0.5}Ni_{0.5})_{68}B_{21.9}Si_{5.1}Nb_5$
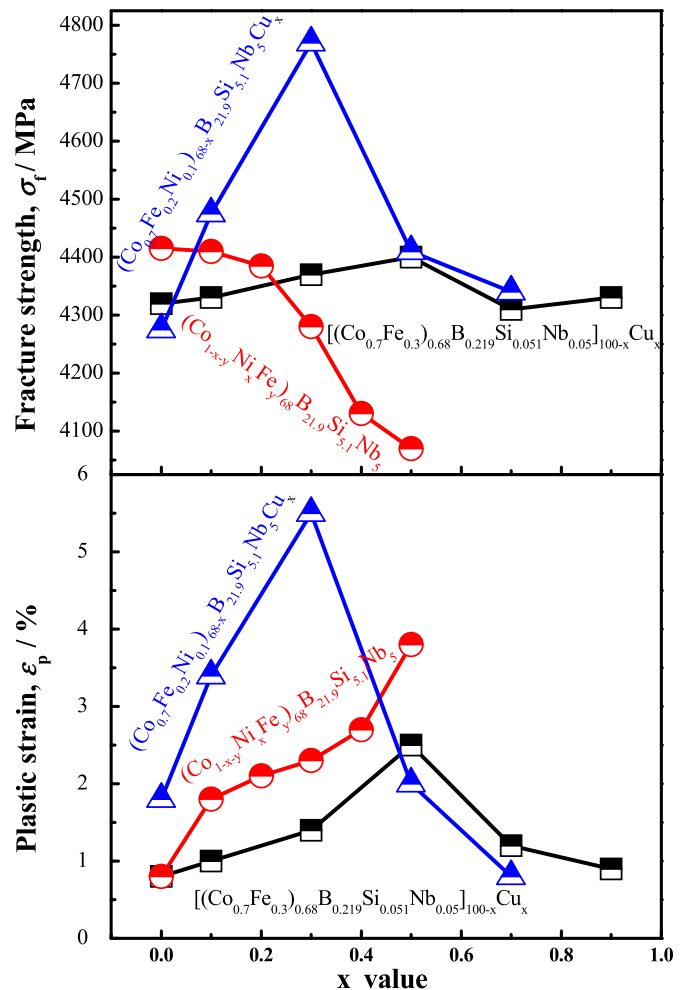
Fig. 7. Comparison of the fracture strength and plastic strain of $[(Co_{0.7}Fe_{0.3})_{0.68}B_{0.219}Si_{0.051}Nb_{0.05}]_{100-x}Cu_x$ ($x = 0$, 0.1, 0.3, 0.5, 0.7, 0.9), $(Co_{1-x-y}Ni_xFe_y)_{68}B_{21.9}Si_{5.1}Nb_5$ ($x = 0$, $y = 0.3$; $x = 0.1$, $y = 0.2$; $x = 0.2$, $y = 0.1$; $x = 0.3$, $y = 0$; $x = 0.4$, $y = 0$; $x = 0.5$, $y = 0$), and $(Co_{0.7}Fe_{0.2}Ni_{0.1})_{68-x}B_{21.9}Si_{5.1}Nb_5Cu_x$ ($x = 0$, 0.1, 0.3, 0.5, 0.7) BMGs.

metallic glass makes it easier to crystallize, which means it is easier to induce structural heterogeneity in the amorphous matrix.

In order to verify the difference in structural heterogeneity of the alloys with varied amount of Ni addition, the nanostructures of $(Co_{1-x-y}Ni_xFe_y)_{68}B_{21.9}Si_{5.1}Nb_5$ (x = 0, y = 0.3; x = 0.5, y = 0) BMGs are compared via TEM analyses, as shown in Fig. 6a and b, respectively. The TEM images of both samples show amorphous nature, and the selected area diffraction (SAED) patterns of these two areas, as shown in the insets of corresponding images, further confirm their amorphous states. However, several areas with 1−2 nm in size that have imperfect translational symmetry can be observed in the TEM images of both samples, as highlighted by the red dashed ellipses. The atomic arrangements of these areas are like nanocrystals, but are too tiny to have diffraction spots shown in the SAED patterns. These areas have been observed in other amorphous alloys before, and defined as crystal-like ordering (CLO) regions [31]. Compared with $(Co_{0.7}Fe_{0.3})_{68}B_{21.9}Si_{5.1}Nb_5$ BMG, the TEM image of $(Co_{0.5}Ni_{0.5})_{68}B_{21.9}Si_{5.1}Nb_5$ BMG has more CLO regions, indicating a higher degree of structural heterogeneity. The structural heterogeneity induced by the CLO regions has positive effects in improving the plastic strain. Firstly, the CLO regions can serve as initiation sites of the STZs at the beginning of plastic deformation during compressive tests, leading to the formation of more shear bands. Besides, during the propagation of shear bands, these CLO regions interact with them, hinder their fast propagation from forming cracks, and induce the formation of multiple secondary shear bands. This is consistent with the morphological observation of the lateral surface of the deformed sample in Fig. 4. As a result, the $(Co_{0.5}Ni_{0.5})_{68}B_{21.9}Si_{5.1}Nb_5$ BMG with an increased degree of structural heterogeneity exhibits a larger plastic strain.

In our previous work, a systematic study of the mechanical performance of $[(Co_{0.7}Fe_{0.3})_{0.68}B_{0.219}Si_{0.051}Nb_{0.05}]_{100-x}Cu_x$ (x = 0, 0.1, 0.3, 0.5, 0.7, 0.9) BMGs was carried out [32], and the variations of fracture strength and plastic strain with Cu addition are summarized and compared with current work, as shown in Fig. 7. We have also investigated the effects of co-addition of Cu and Ni on the mechanical properties of CoFeBSiNb BMG system by producing $(Co_{0.7}Fe_{0.2}Ni_{0.1})_{68-x}B_{21.9}Si_{5.1}Nb_5Cu_x$ (x = 0, 0.1, 0.3, 0.5, 0.7) BMGs (under review), and their fracture strength and plastic strain are also plotted in Fig. 7. According to the data, with increasing Cu addition, both the fracture strength and plastic strain of the BMGs increase first and then decrease. As Cu has large positive mixing enthalpies with Co, Fe, Ni and Nb, proper addition of Cu in the CoFe(Ni)BSiNb BMG system can improve the mechanical performances by introducing atomic-scale structural heterogeneity; however, excessive addition of Cu may result in the formation of large crystals, which reduces not only the plastic strain but also the fracture strength. By contrast, with increasing amount of Ni addition, the changes of the fracture strength and plastic strain are linear; the fracture strength decreases gradually, while the plastic strain increases continuously. The modulation of the mechanical properties in CoFeBSiNb BMGs with Ni addition is through improving v and changing the thermal stability, and only atomic-scale structural heterogeneity (without large crystals formed) can be induced even with a large amount of Ni addition. As discussed before, the amorphous matrix with higher v usually has less icosahedral orderings but more fragmented ones [16], leading to the decrease of yield strength and the improved plasticity. Thus, to obtain Co-based BMGs for applications where that large plasticity is the prerequisite, addition of a large amount of Ni is a promising method.

The magnetic properties of the $(Co_{1-x-y}Ni_xFe_y)_{68}B_{21.9}Si_{5.1}Nb_5$ (x = 0, y = 0.3; x = 0.1, y = 0.2; x = 0.2, y = 0.1; x = 0.3, y = 0; x = 0.4, y = 0; x = 0.5, y = 0) metallic glasses were analyzed. The hysteresis loops are shown in Fig. 8, and the values of B_s and H_c are
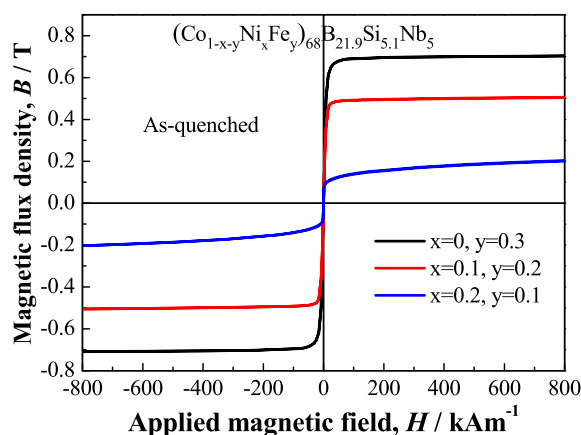

Fig. 8. Hysteresis loops of the $(Co_{1-x-y}Fe_xNi_y)_{68}B_{21.9}Si_{5.1}Nb_5$ (x = 0.3, y = 0; x = 0.2, y = 0.1 and x = 0.1, y = 0.2) metallic glasses measured by VSM.

summarized in Table 1. With increasing amount of Ni substitution for Fe, the B_s decreases gradually from 0.70 to 0.20 T. The reason is that Ni element has only 2 unpaired electrons on 3d-track, leading to its weakest magnetic moment (0.6 μB) compared with that of Fe (2.2 μB) and Co (1.6 μB) [33]. Thus, it results in the decline of B_s with the substitution of Fe with Ni. In addition, it can be found that H_c also decreases gradually from 0.78 to 0.27 A/m with more Ni substitution for Fe. H_c is related to the magnetic anisotropy constant (K) [34]. It was reported that the contribution of Ni (K = 5.7 kJ/m) to K is smaller than that from Fe (K = 48 kJ/m) and Co (K = 410 kJ/m) [35,36]. With more Ni and less Fe/Co, the K value of the metallic glasses decreases gradually, leading to the decrease of H_c. Furthermore, when Fe is completely replaced by Ni, the material changes from ferromagnetic to paramagnetic because of the low atomic magnetic moment of Ni.

4. Conclusion

The effects of Ni substitution for Fe/Co on the mechanical and magnetic properties of Co-based bulk metallic glasses were studied. A $(Co_{0.5}Ni_{0.5})_{68}B_{21.9}Si_{5.1}Nb_5$ BMG with a combination of high strength (4070 MPa) and large plasticity (3.8%) was successfully synthesized. The higher v increases the effective free volume in the alloy and the lower value of G/B hinders fracture and enhances plastic flow. Besides, the lower T_g of this BMG indicates lower shear flow barrier, and the narrower ΔT can easily improve the structural heterogeneity. All of the above effects lead to the increase of plastic flow and the formation of multiple shear bands, thus improving the plasticity of the BMG. The substitution of Fe/Co with Ni leads to the decrease of both saturation magnetization and coercivity of the metallic glasses. When Fe is replaced by Ni completely, the material changes from ferromagnetic to paramagnetic because of the low atomic magnetic moment of Ni. These findings can promote the widespread structural applications of Co-based BMGs with large plasticity.

Author contribution statement

Qianqian Wang: Formal analysis, Writing- Original draft preparation. **Genlei Zhang:** Investigation, Formal analysis. **Jing Zhou:** Validation. **Chenchen Yuan:** Conceptualization. **Baolong Shen:** Writing - Review & Editing, Supervision.

Declaration of competing interest

Acknowledgement

References

[1] P.T. Squire, D. Atkinson, M.R.J. Gibbs, S. Atalay, Amorphous wires and their applications, J. Magn. Magn. Mater. 132 (1994) 10−21.

[2] G. Bordin, G. Buttino, A. Cecchetti, M. Poppi, Temperature dependence of magnetic properties of a Co-based alloy in amorphous and nanostructured phase, J. Magn. Magn. Mater. 195 (1999) 583−587.

[3] B.L. Shen, H. Koshiba, A. Inoue, H. Kimura, T. Mizushima, Bulk glassy $Co_{43}Fe_{20}Ta_{5.5}B_{31.5}$ alloy with high glass-forming ability and good soft magnetic properties, Mater. Trans. 42 (2001) 2136−2139.

[4] A. Inoue, B.L. Shen, H. Koshiba, H. Kato, A.R. Yavari, Cobalt-based bulk glassy alloy with ultrahigh strength and soft magnetic properties, Nat. Mater. 2 (2003) 661−663.

[5] A. Inoue, B.L. Shen, H. Koshiba, H. Kato, A.R. Yavari, Ultra-high strength above 5000 MPa and soft magnetic properties of Co-Fe-Ta-B bulk glassy alloys, Acta Mater. 52 (2004) 1631−1637.

[6] Z.O. Yazici, A. Hitit, Y. Yalcin, M. Ozgul, Effects of minor Cu and Si additions on glass forming ability and mechanical properties of Co-Fe-Ta-B bulk metallic glass, Met. Mater. Int. 22 (2016) 50−57.

[7] J.F. Wang, R. Li, N.B. Hua, T. Zhang, Co-based ternary bulk metallic glasses with ultrahigh strength and plasticity, J. Mater. Res. 26 (2011) 2072−2079.

[8] Z.Q. Liu, W.H. Wang, M.Q. Jiang, Z.F. Zhang, Intrinsic factor controlling the deformation and ductile-to-brittle transition of metallic glasses, Philos. Mag. Lett. 94 (2014) 658−668.

[9] W.M. Yang, H.S. Liu, Y.C. Zhao, A. Inoue, K.M. Jiang, J.T. Huo, H.B. Ling, Q. Li, B.L. Shen, Mechanical properties and structural features of novel Fe-based bulk metallic glasses with unprecedented plasticity, Sci Rep-Uk 4 (2014) 6233.

[10] J. Zhou, W.M. Yang, C.C. Yuan, B.A. Sun, B.L. Shen, Ductile FeNi-based bulk metallic glasses with high strength and excellent soft magnetic properties, J. Alloy. Comp. 742 (2018) 318−324.

[11] J. Zhou, B.A. Sun, Q.Q. Wang, Q.M. Yang, W.M. Yang, B.L. Shen, Effects of Ni and Si additions on mechanical properties and serrated flow behavior in FeMoPCB bulk metallic glasses, J. Alloy. Comp. 783 (2019) 555−564.

[12] S.F. Guo, J.L. Qiu, P. Yu, S.H. Xie, W. Chen, Fe-based bulk metallic glasses: brittle or ductile? Appl. Phys. Lett. 105 (2014).

[13] J. Schroers, W.L. Johnson, Ductile bulk metallic glass, Phys. Rev. Lett. 93 (2004).

[14] X.J. Gu, A.G. McDermott, S.J. Poon, G.J. Shiflet, Critical Poisson's ratio for plasticity in Fe-Mo-C-B-Ln bulk amorphous steel, Appl. Phys. Lett. 88 (2006).

[15] J. Tan, Y. Zhang, B.A. Sun, M. Stoica, C.J. Li, K.K. Song, U. Kuhn, F.S. Pan, J. Eckert, Correlation between internal states and plasticity in bulk metallic glass, Appl. Phys. Lett. 98 (2011).

[16] Y.Q. Cheng, A.J. Cao, E. Ma, Correlation between the elastic modulus and the intrinsic plastic behavior of metallic glasses: the roles of atomic configuration and alloy composition, Acta Mater. 57 (2009) 3253−3267.

[17] G.N. Yang, B.A. Sun, S.Q. Chen, J.L. Gu, Y. Shao, H. Wang, K.F. Yao, Understanding the effects of Poisson's ratio on the shear band behavior and plasticity of metallic glasses, J. Mater. Sci. 52 (2017) 6789−6799.

[18] Y.Q. Dong, Q.K. Man, H.J. Sun, B.L. Shen, S.J. Pang, T. Zhang, A. Makino, A. Inoue, Glass-forming ability and soft magnetic properties of $(Co_{0.6}Fe_{0.3-}Ni_{0.1})_{67}B_{22+x}Si_{6-x}Nb_5$ bulk glassy alloys, J. Alloy. Comp. 509 (2011) S206−S209.

[19] A. Inoue, Stabilization of metallic supercooled liquid and bulk amorphous alloys, Acta Mater. 48 (2000) 279−306.

[20] D. Pan, A. Inoue, T. Sakurai, M.W. Chen, Experimental characterization of shear transformation zones for plastic flow of bulk metallic glasses, P Natl Acad Sci USA 105 (2008) 14769−14772.

[21] M.D. Demetriou, M.E. Launey, G. Garrett, J.P. Schramm, D.C. Hofmann, W.L. Johnson, R.O. Ritchie, A damage-tolerant glass, Nat. Mater. 10 (2011) 123−128.

[22] S.F. Guo, N. Li, C. Zhang, L. Liu, Enhancement of plasticity of Fe-based bulk metallic glass by Ni substitution for Fe, J. Alloy. Comp. 504 (2010) S78−S81.

[23] W.L. Johnson, K. Samwer, A universal criterion for plastic yielding of metallic glasses with a $(T/T_g)^{2/3}$ temperature dependence, Phys. Rev. Lett. 95 (2005).

[24] Z. Liu, K.C. Chan, L. Liu, Enhanced glass forming ability and plasticity of a Ni-free Zr-based bulk metallic glass, J. Alloy. Comp. 487 (2009) 152−156.

[25] B. Sarac, Y.P. Ivanov, A. Chuvilin, T. Schoberl, M. Stoica, Z.L. Zhang, J. Eckert, Origin of large plasticity and multiscale effects in iron-based metallic glasses, Nat. Commun. 9 (2018).

[26] C.C. Yuan, Z.W. Lv, C.M. Pang, X.L. Wu, S. Lan, C.Y. Lu, L.G. Wang, H.B. Yu, J.H. Luan, W.W. Zhu, G.L. Zhang, Q. Liu, X.L. Wang, B.L. Shen, Atomic-scale heterogeneity in large-plasticity Cu-doped metallic glasses, J. Alloy. Comp. 798 (2019) 517−522.

[27] S. Bera, P. Ramasamy, D. Sopu, B. Sarac, J. Zalesak, C. Gammer, M. Stoica, M. Calin, J. Eckert, Tuning the glass forming ability and mechanical properties of Ti-based bulk metallic glasses by Ga additions, J. Alloy. Comp. 793 (2019) 552−563.

[28] J.C. Qiao, Q. Wang, J.M. Pelletier, H. Kato, R. Casalini, D. Crespo, E. Pineda, Y. Yao, Y. Yang, Structural heterogeneities and mechanical behavior of amorphous alloys, Prog. Mater. Sci. 104 (2019) 250−329.

[29] M. Imafuku, C.F. Li, M. Matsushita, A. Inoue, Formation of tau-phase in $Fe_{60}Nb_{10}B_{30}$ amorphous alloy with a large supercooled liquid region, Jpn. J. Appl. Phys. 1 (41) (2002) 219−221.

[30] A. Inoue, B.L. Shen, A new Fe-based bulk glassy alloy with outstanding mechanical properties, Adv. Mater. 16 (2004) 2189−2192.

[31] Q. Wang, C.T. Liu, Y. Yang, J.B. Liu, Y.D. Dong, J. Lu, The atomic-scale mechanism for the enhanced glass-forming-ability of a Cu-Zr based bulk metallic glass with minor element additions, Sci Rep-Uk 4 (2014) 4648.

[32] G.L. Zhang, Q.Q. Wang, C.C. Yuan, W.M. Yang, J. Zhou, L. Xue, F. Hu, B.A. Sun, B.L. Shen, Effects of Cu additions on mechanical and soft-magnetic properties of CoFeBSiNb bulk metallic glasses, J. Alloy. Comp. 737 (2018) 815−820.

[33] L. Ressler, M. Rosenberg, Magnetic-moments and magnetic transitions in the low iron concentration range of the amorphous $Fe_xNi_{80-x}P_{20}$ alloys, J. Magn. Magn. Mater. 83 (1990) 343−344.

[34] G. Herzer, Grain-size dependence of coercivity and permeability in nanocrystalline ferromagnets, IEEE Trans. Magn. 26 (1990) 1397−1402.

[35] S. Chikazumi, Physics of Ferromagnetism, Oxford University Press, Oxford, 1997.

[36] X.D. Fan, Y.T. Tang, Z.X. Shi, M.F. Jiang, B.L. Shen, The effect of Ni addition on microstructure and soft magnetic properties of FeCoZrBCu nanocrystalline alloys, AIP Adv. 7 (2017).